frontiers | Frontiers in Environmental Science

TYPE Original Research
PUBLISHED 09 August 2022
DOI 10.3389/fenvs.2022.937740

Check for updates

OPEN ACCESS

EDITED BY
Buyun Du,
Jiangsu Open University, China

REVIEWED BY
Asheesh Kumar Yadav,
Institute of Minerals and Materials Technology (CSIR), India
Qian Wang,
Shandong Normal University, China
Bhaskar Das,
School of Civil Engineering, India

*CORRESPONDENCE
Shaohong You,
youshaohong@glut.edu.cn
Pingping Jiang,
jiangpp@glut.edu.cn

SPECIALTY SECTION
This article was submitted to Toxicology, Pollution and the Environment, a section of the journal Frontiers in Environmental Science

RECEIVED 06 May 2022
ACCEPTED 18 July 2022
PUBLISHED 09 August 2022

CITATION
Shi Y, Tang G, You S, Jiang P, Zhang X and Deng Z (2022), Treatment mechanism of hexavalent chromium wastewater in constructed wetland-microbial fuel cell coupling system. *Front. Environ. Sci.* 10:937740. doi: 10.3389/fenvs.2022.937740

COPYRIGHT
© 2022 Shi, Tang, You, Jiang, Zhang and Deng. This is an open-access article distributed under the terms of the Creative Commons Attribution License (CC BY). The use, distribution or reproduction in other forums is permitted, provided the original author(s) and the copyright owner(s) are credited and that the original publication in this journal is cited, in accordance with accepted academic practice. No use, distribution or reproduction is permitted which does not comply with these terms.

RETRACTED: Treatment mechanism of hexavalent chromium wastewater in constructed wetland-microbial fuel cell coupling system

Yucui Shi[1], Gang Tang[1], Shaohong You[1,2,3]*, Pingping Jiang[4]*, Xuehong Zhang[1,2] and Zhenliang Deng[1]

[1]College of Environmental Science and Engineering, Guilin University of Technology, Guilin, China, [2]Guangxi Key Laboratory of Environmental Pollution Control Theory and Technology of Guilin University of Technology, Guilin, China, [3]Technical Innovation Center of Mine Geological Environment Restoration Engineering in Southern Stony Hill Area, Nanning, China, [4]College of Earth Sciences, Guilin University of Technology, Guilin, China

RETRACTED

Cr(VI) is toxic to the human body and environment. As a suitable wastewater treatment with low energy requirement technology, constructed wetland-microbial fuel cells (CW-MFCs) can treat Cr(VI) wastewater while generating electricity. In this study, CW-MFC and constructed wetland systems were developed to purify Cr(VI) wastewater. The removal mechanism of Cr(VI) was examined by electron paramagnetic resonance (EPR), X-ray photoelectron spectroscopy (XPS), and Fourier transform infrared spectroscopy. The results demonstrated that the average pollutant removal efficiency of the CW-MFC system is 2.99–8.13% higher than that of the constructed wetland system, and the maximum power density is 505.61 mW m^{-2}. Moreover, the XPS and EPR analyses demonstrated that Cr in substrates and *Leersia hexandra* Swartz primarily is in the form of Cr(III). Moreover, in plants and substrates, the Cr(III) content of the CW-MFC system was higher than that of the control, and the bioconcentration and translocation factors were 0.23 and 0.05 higher than those in the control group, respectively. Therefore, the CW-MFC system can efficiently remove Cr(VI) and promote the accumulation and transport of Cr. Microbial community diversity in the CW-MFC was significantly higher than CW. The abundance of electrogenic bacteria Geobacter and metal dissimilatory reducing bacteria *Acinetobacter* in CW-MFC is higher than that in CW. To summarize, the study results provide a theoretical basis for the mechanism study of Cr(VI) wastewater treatment using CW-MFC systems.

KEYWORDS

CW, MFC, *Leersia hexandra* Swartz, wastewater treatment, XPS, FTIR, EPR

Abbreviations: COD, chemical oxygen demand; CW, constructed wetland; EPR, electron paramagnetic resonance; FTIR, Fourier transform infrared spectroscopy; MFC, microbial fuel cell; XPS, X-ray photoelectron spectroscopy.

1 Introduction

In the last many decades, hexavalent Cr has been extensively used in the welding, tanning, mining, electroplating, and pigment industries (Li et al., 2018). Because of its wide range of industrial applications, Cr is one of the primary toxic heavy metals. (Dermou et al., 2005). Therefore, the chemical reduction of Cr(VI) to Cr(III) is an acceptable and effective technology, as it can reduce Cr(VI) toxicity and stability in polluted environments. Generally, the moderate intake of Cr(III) is beneficial to the human body, whereas Cr(VI) has high solubility, fluidity, and toxicity (mutagenicity, carcinogenicity, and teratogenicity) (Gil-Cardeza et al., 2014; Qin et al., 2016). The long-term exposure to Cr(VI) may cause serious health problems, such as stomach and skin tumors and liver and kidney damage, and lead to interferences with the DNA transcription process (Vendruscolo et al., 2017; Li et al., 2018). Unlike certain organic pollutants, Cr(VI) is non-biodegradable and can be stored in the environment for long periods of time (Li et al., 2012). Moreover, Cr(VI) is relatively stable in water, exists in a dissolved state, has a strong migration ability in the environment, and can be reduced to Cr(III) under certain conditions. Cr(III) can be easily adsorbed by the bottom sludge in water, where most of it is transferred to the solid phase and only a small amount is dissolved in water. The hydrolysis of Cr(III) produces a precipitate of chromium hydroxide; however, Cr(III) was adsorbed by water particles and precipitated into the sediment, thus resulting in a weak migration of Cr(III) in water (Blowes 2002). Therefore, Cr(VI) has been listedas a priority pollutant in many countries around the world (Broadway et al., 2010; Barrera-Díaz et al., 2012).

Presently, the Cr(VI) removal methods primarily include ion exchange (Dharnaik and Ghosh 2014), filtration (Kazemi et al., 2018), advanced redox (Sinha et al., 2017), adsorption (Sun et al., 2014; Adam et al., 2018), microbial adsorption (Zheng et al., 2019), and electrochemistry (Zongo et al., 2009). However, these methods have limitations, including low treatment levels and high investment and operation costs (Chaudhry et al., 2017). Moreover, they are unsuitable for treating polluted water bodies with large area and low concentration of Cr(VI). Constructed wetland (CW) has a number of complex ecosystems, including plants, microorganisms, substrates, and water. Moreover, it has a high treatment capacity for heavy metals, such as Cr, and the refractory organics in wastewater (Dotro et al., 2012; Gomes et al., 2018). Microbial fuel cells (MFCs) have been extensively examined as a new technology for purifying wastewater while generating electricity (Gul P. et al., 2021; Uddin et al., 2021). Certain studies used transition metals, such as Cu(II) (Tao et al., 2011), Ag(I) (Choi and Cui 2012), and Hg(I) (Wang et al., 2011), as electron acceptors, but their success rates were limited. Note that the oxidation–reduction potential of Cr(VI) (1.33 V) is higher than that of O_2 (1.23 V) (Gupta et al., 2017; Li and Zhou 2018; Ren et al., 2018). Therefore, Cr(VI) can be used as an electron acceptor and be converted to Cr(III).

Because both CW and MFC can remove Cr in water, the redox gradient of the natural layering of the CW system is highly consistent with the operating conditions of MFC, thus providing the feasibility for the coupling of CW and MFC systems (Yadav et al., 2012). In recent years, the ability of constructed wetland-microbial fuel cell (CW-MFC) systems to provide low electricity while improving the treatment capacity of heavy metal wastewater has attracted considerable attention (Wang et al., 2022). A removal study of Pb(II) by CW-MFC displayed that the removal efficiency was up to 85% with a maximum power density of 7.432 mW m^{-3} (Zhao et al., 2020). In another study, approximately 91% removal of Cr(VI) was obtained in CW-MFC under the optimal operating conditions (Mu et al., 2020). However, the current research is only aimed at improving the treatment capacity of Cr(VI) (Srivastava et al., 2020a), and the removal mechanism of Cr(VI) in water by CW-MFC system is still not very clear. Therefore, to investigate the redox properties of Cr in CW-MFC systems, this study combines physical adsorption, bioelectrochemical reduction, and microbiological research methods for remove Cr(VI) from water bodies and evaluate the comparison of the treatment ability of CW-MFC and CW systems on the Cr(VI) polluted wastewater. Electron paramagnetic resonance (EPR), X-photoelectron spectroscopy (XPS), Fourier transform infrared spectroscopy (FTIR) were used to analyze the quality of wetland effluent, valence state of chromium, and chemical characteristics of Cr in wetland matrices and plants. The biogeochemical mechanisms of Cr(VI) for water treatment were discussed and compared, focusing on providing a scientific basis for improving the

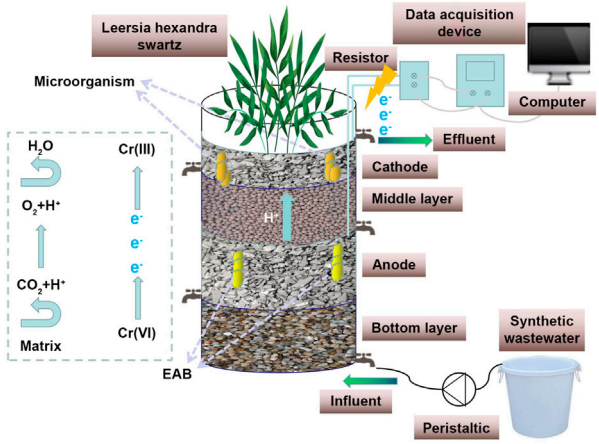

FIGURE 1
Installation diagram of the constructed wetland-microbial fuel cell coupling system (EAB, electrochemically active bacteria).

RETRACTED

treatment performance of Cr(VI) purified water in CW-MFC coupling systems.

2 Material and methods

2.1 System construction and sludge inoculation

A vertical upward-flow CW-MFC sewage treatment system was constructed for this study. The primary part comprises a reactor made of UPVC pipes with a diameter of 30 cm, a height of 70 cm, and an effective height of 60 cm (Figure 1). A water inlet is located at the bottom of the system, and a water outlet lies close to the top at a height of 60 cm. The system is composed of a bottom layer (zeolite, 15 cm), an anode layer (activated carbon, 20 cm), and a middle layer (ceramsite, 15 cm), as well as a cathode layer (activated carbon, 10 cm). Both anode and cathode are composed of 100-mesh-sized stainless steel wrapped with activated carbon. The design of the stainless steel mesh improves the contact area between the MFC and the pollutants, as well as prevents the irregular diffusion of electrons, which improves the power generation performance of the system. The anode and cathode wires are connected by a copper wire and an external resistance box (Fuyang Precision Instrument Factory, Hangzhou, China). The voltage information is collected using an information acquisition card (NI USB-6009, Suzhou Fuyutong Electronics Co., Ltd., China). The source of inoculation is concentrated anaerobic sludge from Guilin Liquan Brewery. The anaerobic sludge is first acclimated in a laboratory anaerobic reactor for a week and then transferred to each reactor. Each system is inoculated with sludge for 2 months. The system uses artificially prepared Cr(VI) wastewater. *Leersia hexandra* Swartz is the wetland plant (*L. hexandra* is the first wet chromium hyperaccumulator found in China), and the cathode and anode of the system control group are not connected to the resistance box. After a preliminary simulation experiment, the experiment were conducted with a COD concentration of 300 mg L^{-1}, a Cr(VI) concentration of 80 mg L^{-1}, and artificially simulated Cr(VI) wastewater with a pH of 6.5–8.0.

2.2 Analytical methods

2.2.1 Determination of heavy metal chromium and a valence state analysis

After wetland operation, substrates were sampled using a five-point sampling method by inserting a sampler into the wetland system, maintaining the same depth and mass of each matrix sample. The collected samples are placed in an oven at 75°C, baked to a constant weight, grated, and then set aside after a 100 mesh-sized sieve. A part of the samples was used for determining the Cr content, and the other part was used for XPS and FTIR detection. The roots, stems, and leaves of *L. hexandra* were collected, washed, and then placed in an oven at 105°C for 30 min. Then, they were dried at 75°C to constant weight and used for EPR detection after crushing. The roots, stems, leaves, and the Cr(VI) substrate were extracted using the basic digestion method (EPA3060A), and Cr(VI) obtained after the extraction process was determined using the water quality–determination of chromium(VI)–1,5 diphenylcarbohydrazide spectrophotometric method. The extraction of total Cr was performed using the acid digestion method, and Cr obtained after the digestion process was determined by the water quality–determination of chromium–flame atomic absorption spectrometry. The measurement experiments were set up using three parallel samples, and the average experimental results were obtained.

In this study, Bioconcentration factor (BCF) refers to the ratio of the content of the Cr content of plants to the corresponding element content in the substrate cathode. The higher BCF value indicates that the plant has a higher capacity to absorb heavy metals. Transfer factor (TF) refers to the ratio of the content of heavy metals in the aboveground to the belowground heavy metal content. The larger TF, the more heavy metals can be transferred from the roots to the above-ground parts. Substrate and plant morphological analyses are as follows:

XPS test steps: Take an appropriate amount of sample and press it, stick it on the sample tray, and put the sample into the sample chamber of the Thermo Scientific K-Alpha XPS instrument. When the pressure of the sample chamber is less than 2.0×10^{-7}mbar, send the sample into the analysis chamber. The spot size was 400 μm, the working voltage was 12 kV, and the filament current was 6 mA; the full-spectrum scanning pass energy was 150 eV with a step size of 1 eV; the narrow-spectrum scanning pass energy was 50 eV with a step size of 0.1 eV.

FTIR test steps: In a dry environment, take a sample visible to the naked eye and an appropriate amount of dry potassium bromide powder into a mortar, and grind it for several times. Then put it into the tablet machine for tableting (press into a transparent sheet). During the test, the background was collected first, and then the infrared spectrum of the sample was collected. The resolution was 4 cm^{-1}, the number of scans was 32 times, and the test wavenumber range was 400–4,000 cm^{-1}.

EPR test steps: Disperse the solid sample ultrasonically in the corresponding solvent, prepare a solution of 1 mg mL^{-1}, take an equal amount of the dispersion and mix with the capture agent, and then use a capillary to absorb an appropriate amount of the mixture, put it into a quartz tube, and insert it into the sample cavity. After adjusting the instrument, set the parameters, start scanning the spectrum, and save the data.

2.2.2 Water quality analysis indicators

After stabilization of the system, the samples were regularly obtained from each reactor as per experimental conditions. All samples to be tested were passed via a 0.45-μm-sized glass fiber

RETRACTED

filter membrane to remove any suspended impurities before the measurements. COD was determined using the water quality–determination of the COD-dichromate method (HJ828-2017). Ammonia nitrogen was determined using the water quality–determination of ammonia nitrogen-Nessler's reagent spectrophotometry (HJ535-2009). Total phosphorus was determined using the water quality–determination of total phosphorus–ammonium molybdate spectrophotometric method (GB11893-89). Cr(VI) was determined using the solid waste–determination of chromium(VI)-1,5-diphenylcarbohydrazide spectrophotometric method (GB7467-87). The pollutant removal efficiency R_E could be calculated using the following Formula 1:

$$R_E = \frac{C_{in} - C_{out}}{C_{in}} \times 100 \quad (1)$$

In the formula, R_E is the pollutant removal efficiency, C_{in} is the CW-MFC pollutant influent concentration, and C_{out} is the CW-MFC pollutant effluent concentration. The unit of COD is mgL^{-1}.

2.2.3 Electrochemical analysis index

Voltage collection: The data collection card (NI USB-6009, Suzhou Fuyutong Electronics Co., Ltd., China) collects voltage information, it was connected to a computer to realize online real-time monitoring. The sampling frequency was 15 min, and the sampling period was determined as follows: the actual operation requirements of the device. The current in the circuit was calculated using Ohm's law, as shown in Formula 2:

$$I = \frac{U}{R} \quad (2)$$

In the formula, I is the current (mA), U is the voltage (mV), and R is the external resistance (Ω).

Power density curve and polarization curve: Perform the measurements when the battery is stably working. First, place the circuit on for ~ 24 h. After stabilizing, record the open-circuit voltage. Then, reduce the resistance value from 10,000–10 Ω every 15 min (i.e., 10,000, 8,000, 6,000 . . . 50, 10). Record the voltage value across the resistor after the system stabilizes at each resistance value. The current is calculated using Ohm's law from the measured battery voltage. Then, calculate the current density I_A 3) and power density P_A 4) as per the following formulas and then draw the power density curve and polarization curves.

$$I_A = \frac{U}{R \times A} \quad (3)$$

In the formula, I_A is the current density (mAm^{-2}), U is the voltage (mV), R is the external resistance (Ω), and A is the effective area of the anode (m^2).

$$P_A = \frac{U \times I}{A} \quad (4)$$

In the formula, P_A is the power density (mWm^{-2}), U is the voltage (mV), I is the current (mA), and A is the anode effective area (m^2).

MFC internal resistance: This study used the polarization curve slope method to obtain the internal resistance of the CW-MFC system, i.e., the slope of the linear section of the polarization curve is the internal resistance.

2.3 Scanning electron microscopy

Before the system is operated, the original activated carbon is collected and stored in dry environment. After the system was stabilized, samples of the cathodic activated carbon and anodic activated carbon were collected. The plant sample was oven-dried at 75°C. The dried sample was then ground and was made to pass through a 200 mesh-sized sieve to obtain uniform particle size. The activated carbon sample uses scanning electronic microscope to observe the form of the electrode biofilm pattern. The specific steps are as follows:

Take the trace solid sample directly to the conductive glue, and use the Oxford Quorum SC7620 sputtering coating instrument to spray 45s, the spray gold is 10mA; then use the scanning electron microscope (SEM, ZEISS Sigma 300/ZEISS GeminiSEM 300/TESCAN MIRA LMS, Germany) to shoot the sample appearance. The acceleration voltage was 3 kV during topography shooting. The detector is the second electronic detector of the SE2.

2.4 Microbial community analysis

While operating the experimental system, the system filler was sampled as per the experimental requirements, 16S rRNA gene sequencing was used, and 454 high-throughput sequencing technology was used to analyze the microbial community structure. The filler samples were extracted and placed in sampling bottles during sampling, stored in ice packs during transportation to the laboratory, and then stored in a -80°C refrigerator for sequencing by Sangon Biotech (Shanghai) Co., Ltd., After sampling, the kit was first used for DNA extraction, followed by amplification and purification of the 16sRNA gene fragment in the V3-V4 region, and finally 454 high-throughput sequencing.

2.5 Quality control

In order to ensure the accuracy of the test results, the instrument components were cleaned and debugged before the test. Based on the concentration of the standard solution and the solution to be tested, the error of the instrument was taken to be three times the detection limit. One quality control

RETRACTED

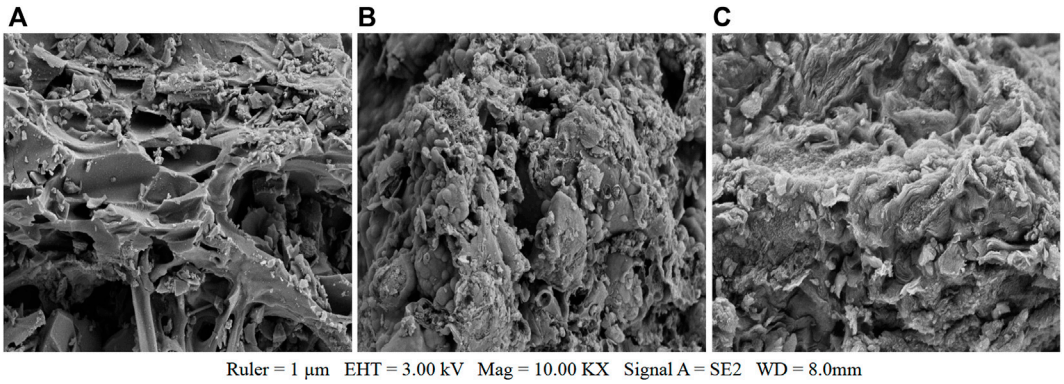

FIGURE 2
Surface morphology and microstructure of **(A)** virgin activated carbon, **(B)** anode biofilm, and **(C)** cathode biofilm of constructed wetland-microbial fuel cell.

sample was added for every 10 samples, and the recovery rate of heavy metals in quality control samples was 90–110%.

3. Results and discussion

3.1 Scanning electron microscopy

The figure shows the surface structure of the original activated carbon and the anode and cathode activated carbon after coating (Figure 2). The surface of the original activated carbon is relatively rough and has many inhomogeneous layers of pores, which creates beneficial living conditions for bacterial growth and improving the possibility of heavy metal adsorption (Gul H. et al., 2021; Hanumantu 2021). Compared with the original activated carbon, a dense biofilm was formed on the surface of the activated carbon after film hanging. Studies demonstrated that the microorganisms acting as biocatalysts can oxidize carbon sources and promote electricity generation (Mu et al., 2020). Furthermore, the surface of the activated carbon was covered with metal ions, and the pores were relatively smooth. This may have occurred because of the reduction in the inhomogeneity of the adsorbent surface. This observation indicates that metals are adsorbed on the functional groups within pores (Hanumantu 2021). Therefore, the CW-MFC system ran stably during the experiment.

3.2 Treatment and power generation of the Cr(VI) wastewater

Figure 3 shows that the pollutant removal efficiency of the CW-MFC system is on an average 2.99–8.13% higher than that of the control group. The pollutant removal efficiency and system voltage increased with the extension of the wetland system operation time and were eventually stabilized (Figure 4A). As the external resistance was sequentially reduced from 10,000–10 Ω, the maximum voltage of the system was 499 mV, and the maximum power density was 505.61 mW m^{-2} (Figure 4B). The organic matter in the CW-MFC system was oxidized to electron donors using the electrochemically active microorganisms on the anode (Logan and Regan 2006). Moreover, the presence of the external circuit promoted electron transfer, stimulated the growth of microorganisms in the anode area and increased the oxidation–reduction reaction rate, thereby achieving the removal effect (Srivastava et al., 2020b; Gupta et al., 2021). As per the research of Zhao et al. (Zhao et al., 2020), the microbial diversity and community richness were generally higher in CW-MFC than in CW. Hartl et al. (Hartl et al., 2019) also reported similar results, and they demonstrated that the pollutant removal efficiency of closed-circuit systems is higher than that of the open-circuit systems.

3.3 Chromium distribution and accumulation

The total chromium and Cr(III) accumulated by *L. hexandra* in the CW-MFC system were higher by 3582.29 and 4,326.04 mg kg^{-1}, respectively, and the Cr(VI) content was lower by 743.75 mg kg^{-1} (Table 1). The total chromium and Cr(III) contents in the substrates were 2928.13 mg kg^{-1} and 3352.71 mg kg^{-1}, respectively, which is higher than the CW system, and the content of Cr(VI) was 424.58 mg kg^{-1}, which was lower than the CW system (Table 2). As shown in Table 3 that the plant–heavy metal BCF of the CW-MFC system was 0.23, higher than that of the control group, and that the TF was 0.05, higher than that of the control group. Most of the chromium entering the wetland system was trapped in the

RETRACTED

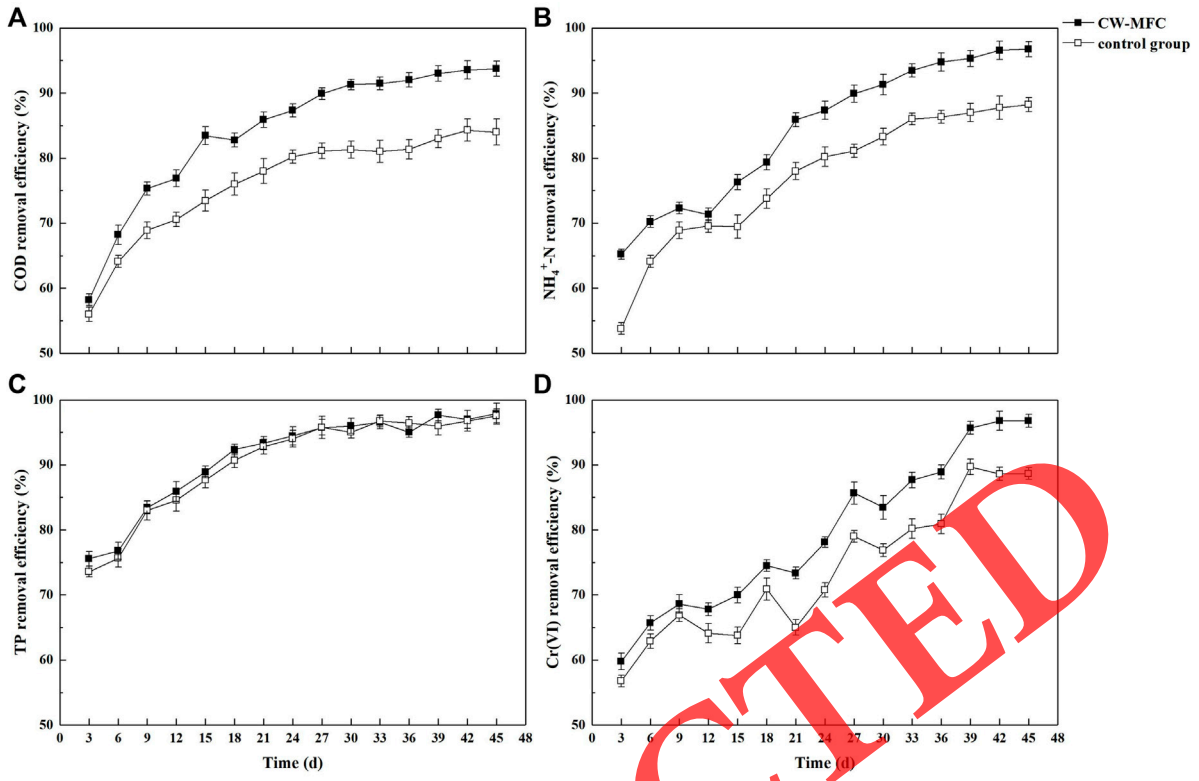

FIGURE 3
Constructed wetland-microbial fuel cell (CW-MFC) and CW removal efficiency of system pollutants: **(A)** Chemical oxygen demand (COD) removal efficiency, **(B)** NH_4^+-N removal efficiency, **(C)** total phosphorus (TP) removal efficiency, **(D)** Cr(VI) removal efficiency.

RETRACTED

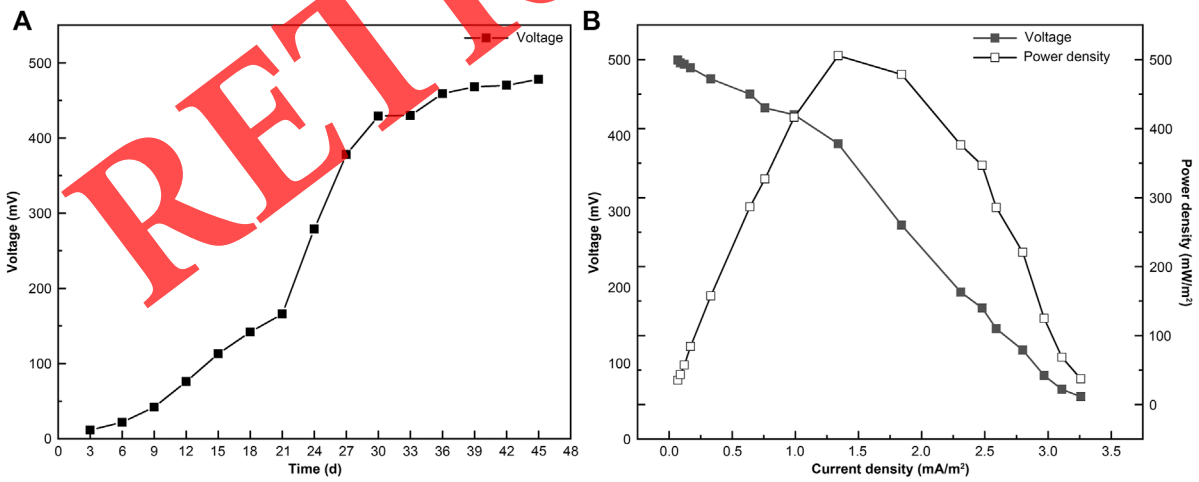

FIGURE 4
Constructed wetland-microbial fuel cell (CW-MFC) system power generation: **(A)** CW-MFC system voltage, **(B)** power density curve and polarization curve of the CW-MFC system.

TABLE 1 Cr concentrations in the plants.

	Total chromium (mg·kg^{-1})			Total chromium of plant (mg·kg^{-1})	Cr(VI) (mg·kg^{-1})			Cr(VI) of plant (mg·kg^{-1})	Cr(III) (mg·kg^{-1})			Cr(III) of plant (mg·kg^{-1})
	Root	Stem	Leaf		Root	Stem	Leaf		Root	Stem	Leaf	
CW-MFC	8969.79	2100	1t934.38	13004.17	1406.25	614.58	770.83	2791.66	7563.54	1485.42	1163.54	10212.5
Control group	6752.08	1428.13	1241.67	9421.88	2320.83	662.5	552.08	3535.41	4431.25	765.63	689.58	5886.46

TABLE 2 Cr concentrations in the substrates.

	Total chromium (mg·kg^{-1})		Cr(VI) (mg·kg^{-1})		Cr(III) (mg·kg^{-1})	
	Anode	Cathode	Anode	Cathode	Anode	Cathode
Constructed wetland-microbial fuel cell	4977.08	5911.46	413.33	182.92	4563.75	5728.54
Control group	3189.58	4770.83	572.50	448.33	2617.08	4322.50

TABLE 3 Bioconcentration and translocation factors.

	Bioconcentration factor	Translocation factor
Constructed wetland-microbial fuel cell	2.20	0.45
Control group	1.97	0.40

RETRACTED

substrate, whereas the chromium accumulated in the plants was primarily concentrated in the roots of *L. hexandra*. This indicates that substrates (Chen et al., 2020) and plants (Han et al., 2008) play an important role in the fixation and removal of Cr (Liu et al., 2014). This study reported that the micro-current environment is beneficial to the growth of plants to a certain extent (Zhou et al., 2017). As shown in this figure, both anode and cathode can adsorb a certain amount of Cr(VI) and Cr(III), however, the cathode can adsorb more Cr. This confirms that the primary removal route of Cr in *L. hexandra* CW-MFC is cathode bioelectrochemical reduction of Cr(VI) to Cr(III) and Cr(III) precipitation (Habibul et al., 2016). Compared with CW, *L. hexandra* produces more biomass, accumulates more heavy metals, while also generating more bioelectricity and improve the activity of aerobic microorganisms, thus promoting the removal of pollutants (Di et al., 2020). Briefly, plant biomass and electrical performance were mutually reinforcing. Studies demonstrated that the root tissues of gramineous plants, such as *L. hexandra*, can secrete iron-deficient mugineic acids, which can increase the absorption efficiency of metal elements in roots (Römheld 1991). The results of Liu et al. (Liu et al., 2022) demonstrated that the removal of Cr(VI) was primarily performed by the adsorption and accumulation of the substrate, while the concentration of enriched chromium in plants was less than substrate and water, and the enriched chromium was primarily concentrated in the roots of plants.

As per the abovementioned results and analysis, Cr(VI) in *L. hexandra* CW-MFC can be removed by combining bioelectrochemical reduction, plant accumulation and precipitation, in which the bioelectrochemical reduction process is the primary mechanism for Cr(VI) removal. The bioelectrochemical reduction of Cr(VI) reduces the toxicity of Cr(VI) to plants and promotes the absorption of Cr by plants, thereby improving the removal efficiency of Cr(VI) in wastewater.

3.4 Morphological characteristics of chromium

3.4.1 Morphological characteristics of the chromium in substrates

It can be seen from Figure 5 that the primary peaks observed at 285.08 and 531.08 eV correspond to C and O, respectively. C is generated by exposure to small molecules in carbon dioxide, air, and water. The peak position of O is attributed to the high oxygen content of the system's cathode, and it is classified as the peak of surface chemisorption oxygen (Wang et al., 2022), and the other elements may exist in the form of oxides or hydroxides (Liu et al.,

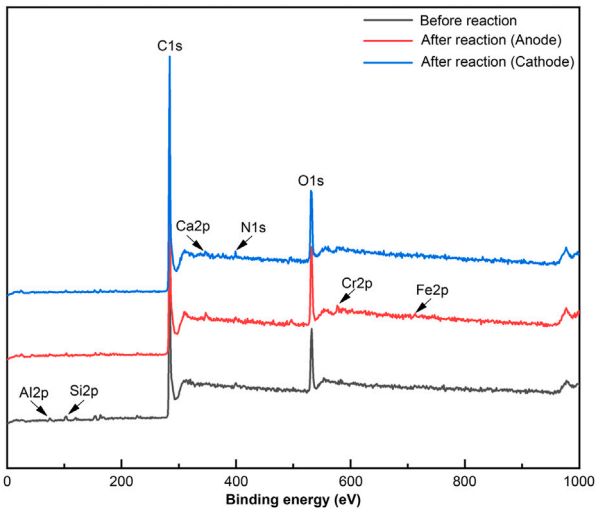

FIGURE 5
X-ray photoelectron spectroscopy wide scan spectra of the substrates.

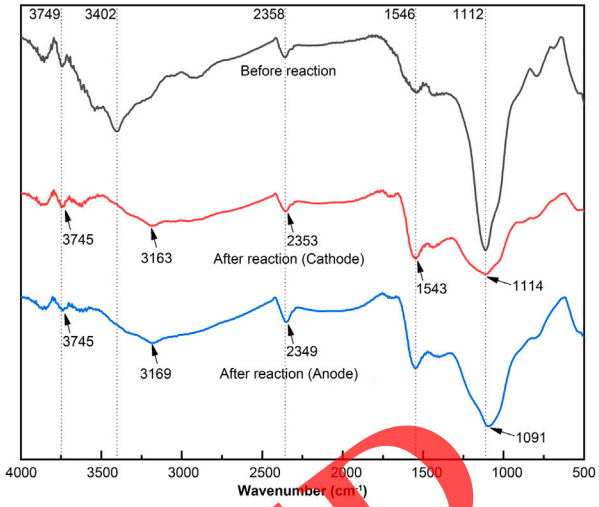

FIGURE 7
Fourier transform infrared spectroscopy spectra of the substrates.

2014). Furthermore, the added peak detected at 577.08 eV can be attributed to the Cr2p peak. These results demonstrate that the activated carbon surface contained Cr after the reaction in the CW-MFC system.

In the Cr2p spectrum of the CW-MFC system, the characteristic peaks corresponding to Cr(III) were 577.48 eV (anode) and 577.30 eV (cathode), respectively, and the characteristic peaks corresponding to Cr(VI) were 579.67 eV (anode) and 579.60 eV (cathode), respectively. As per the peak area, the anode and cathode Cr(III) contents were 85.40 and 93.63%, respectively, whereas the anode and cathode Cr(VI) contents were 14.60 and 6.37%, respectively (Figure 6). The results demonstrated that 85.40% of Cr(VI) was reduced to Cr(III) in the anode, which may be by Cr-reducing microorganisms. The cathode can reduce more Cr(VI), and the chemical and microbial processes may cause a reduction in Cr(VI) (Moreau et al., 2013), which confirms that the cathode bioelectrochemical reduction

RETRACTED

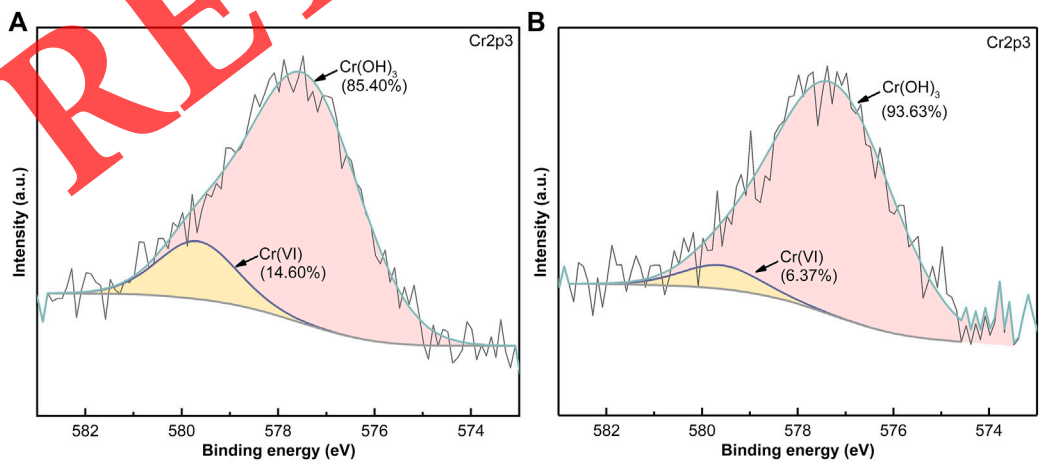

FIGURE 6
High-resolution X-ray photoelectron spectroscopy spectra of Cr2p3 after the adsorption of Cr(VI) by the constructed wetland-microbial fuel cell system: **(A)** anode, **(B)** cathode.

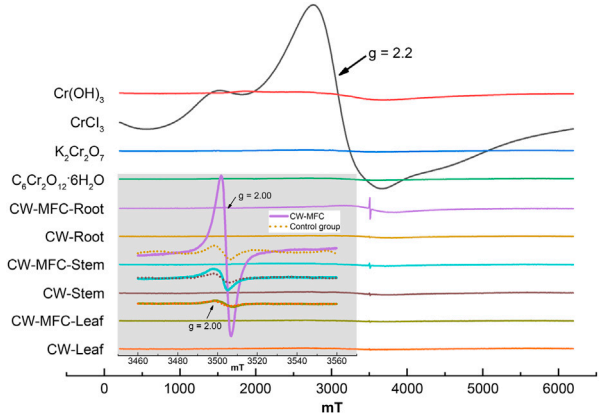

FIGURE 8
L. hexandra's electron paramagnetic resonance spectra of the constructed wetland-microbial fuel cell (CW-MFC) and CW systems.

reaction is the primary route of Cr removal in *L. hexandra* CW-MFC. The presence of C, O, and Fe reported that Cr in substrates can exist in organic Cr(III) complexes or Cr(III)–Fe(III) hydroxides (Kotaś and Stasicka 2000; Liu et al., 2014). Although the method used in this study cannot confirm the Cr species, Cr(III) can be hydrolyzed to $Cr(OH)_3$ under neutral or alkaline conditions (Blowes 2002).

It can be seen from Figure 7 that the FTIR spectra before and after the reaction are similar, indicating that the structure was similar. After the matrix adsorbed Cr(VI), the absorption peaks at the anode and cathode at 3402 cm^{-1} moved 233 cm^{-1} and 239 cm^{-1} to the low wavenumber region, respectively. Moreover, the absorption peak at 2358 cm^{-1} moved 9 cm^{-1} and 5 cm^{-1} to the low wavenumber region, respectively, and the absorption peak at 1546 cm^{-1} moved 3 cm^{-1} to the low wavenumber region. The absorption peak at 1112 cm^{-1} at the anode moved 8 cm^{-1} to the low wavenumber area, whereas the absorption peak at the cathode moved 2 cm^{-1} to the high wavenumber area. This shows that the -OH (Lim et al., 2008), $-NH_2$, C=N (Ren et al., 2016), C=C, N=O, and C–O(Lim et al., 2008) groups are related to the adsorption and reduction of chromium (Jain et al., 2010). Both cathode and anode showed obvious shoulder-structures at wavenumbers of 1100–1800 cm^{-1}, which was usually attributed to multiple oxygen-containing functional groups (Yangdong et al., 2012). During the whole process of electricity generation, electroactive bacteria secrete a large amount of cytochrome C, and its structure has a large number of oxygen-containing functional groups such as carboxyl and amide groups. Therefore, the abundance of oxygen-containing functional groups in the FTIR spectrum may be related to the secretion of cytochrome C (Li et al., 2019). These results suggest that organics in the matrix participate in the reduction of Cr(VI) while acting as electron donors to generate electricity.

3.4.2 Morphological characteristics of chromium in plants

The EPR spectra of the reference materials $K_2Cr_2O_7$ and $C_6Cr_2O_{12}·6H_2O$ demonstrated no obvious characteristic peaks in the entire magnetic field. The EPR spectra of $CrCl_3$ and $Cr(OH)_3$ showed obvious signal areas at g = 2.00, as shown in Figure 8. The EPR spectrum of *L. hexandra*'s roots, stems, and leaves demonstrated characteristic peaks at g = 2.00. These g values agreed with the g values of the standard materials $CrCl_3$ and $Cr(OH)_3$ in the obvious signal area, indicating that the Cr in the roots, stems, and leaves of *L. hexandra* primarily is in the form of Cr(III). Furthermore, compared with the CW system, the EPR signal amplitude of plants in the CW-MFC system was larger. This indicates that the Cr(VI) reduction in plant tissues was more intense (Howe et al., 2003). This may be because electron transfer changes the metabolic state of plants, promotes the synthesis of the redox compounds in plants, and reduces Cr(VI) to Cr(III). There were also thiol S(II) compounds known as abiotic stress factors (Dubey et al., 2010). These results were consistent with the results of Augustynowicz et al. (Augustynowicz et al., 2013). Using EPR to measure hexavalent Cr reduction could also be performed on other aquatic plants (Espinoza-Quiñones et al., 2008; Augustynowicz et al., 2014). However, these species undergo the reduction of Cr(VI) after the further biological absorption of Cr(III) in roots and leaves. Thus, the roots are primarily responsible for isolating Cr and other metals (Padmavathiamma and Li 2007).

4. Microbial community structure analysis

4.1 Community diversity analysis

As shown in Table 4, the higher Chao1 index and Ace index indicated the microbial community was more abundant. The higher the Shannon index, the lower the Simpson index and the higher the community diversity. The analysis of Alpha diversity index demonstrates that bioelectricity production in the CW-MFC system is more conducive to the growth and reproduction

TABLE 4 Statistics of alpha diversity index.

Sample	Number	OTUs	Shannon	Chao	Ace	Simpson	Shannonven
CW-MFC	61597	1457	5	1748.26	1713.75	0.03	0.69
CW	59773	1325	4.59	1256.55	1287.06	0.06	0.61

RETRACTED

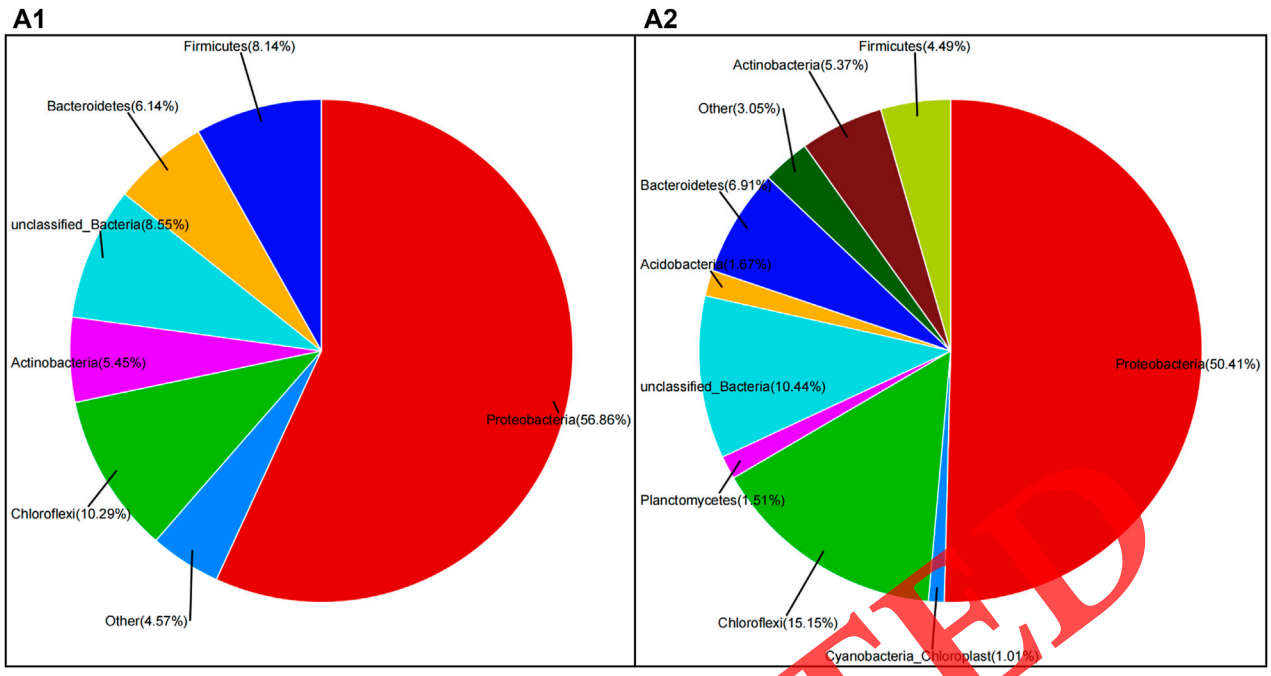

FIGURE 9
Relative abundance map of microbial community composition at CW-MFC and CW phylum levels: **(A1)** CW-MFC system, **(A2)** CW system.

RETRACTED

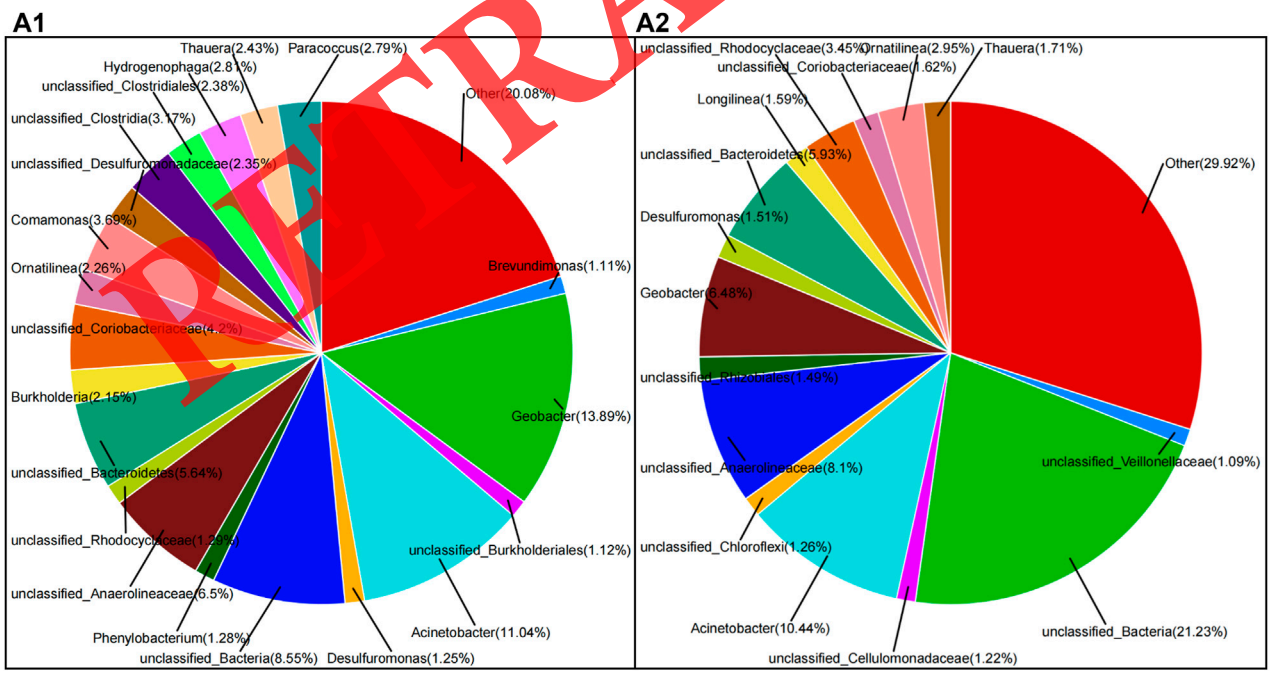

FIGURE 10
Relative abundance map of microbial community composition at CW-MFC and CW genus levels: **(A1)** CW-MFC system, **(A2)** CW system.

of microorganisms, as well as has a positive effect on the increase of community diversity (Torresi et al., 2017; Tao et al., 2020).

4.2 Analysis of system community composition

Figure 9 shows the microbial community composition of CW-MFC and CW at the phylum level. The microbial proportions of CW-MFC and CW systems are Proteobacteria (56.86 and 50.41%), Chloroflexi (10.29%, 15.15%), Bacteroidetes (6.14%, 6.91%), Actinobacteria (5.45%, 5.37%), and Firmicutes (8.14%, 4.49%). Previous studies demonstrated that both Proteobacteria and Firmicutes were defined as the most common EABs in MFC reactors(Logan and Regan 2006; Wang et al., 2019; Tao et al., 2020). The microorganisms of various genera in the Proteobacteria phylum play important roles in degrading substrates and generating electricity (Obata et al., 2020). Cheng et al. (Cheng et al., 2021) noted that the high EAB abundances in both devices would have promoted COD removal, and the results confirmed that this did occurred. The three most common microbe phyla in the CW-MFC were Proteobacteria, Firmicutes, and Bacteroidetes. In this study, the total content of these three microbe phyla in the CW-MFC system was higher than that in the CW system. Xie et al. (Xie et al., 2017) found similar results.

Figure 10 shows the microbial taxa in the system are classified at the genus level. Common genera identified by CW-MFC and CW primarily included *Acinetobacter* (11.04%, 10.44%), Geobacter (13.89%, 6.48%), Thauera (2.43%, 1.71%), and Desulfuromonas (1.25%, 1.51%). Pradhan et al. (Pradhan et al., 2017) has been demonstrates that *Acinetobacter*, a bacterium tolerant to many metals and oxygen-consuming pollutants, has been used for Cr(VI) removal and has shown good chromium-reducing ability. Geobacter was the most common electrogenic microorganism in MFC, and the energy conversion rate of Geobacter metallireducens was as high as 25.8% (Jiang et al., 2009). Geobacter's nanowire structure could achieve direct contact with electrodes and conduct electrons to electrodes, thus reducing electron loss when conducting via other electron mediators, and generating better electricity (Reguera et al., 2005; Gorby et al., 2006). Moreover, Wang et al. (Wang et al., 2019) believed that Desulfuromonas were the possible EAB. Therefore, the relative abundance of Geobacter in CW-MFC contributed to the high power generation. Thauera was an autotrophic denitrifying bacteria (Mousavi et al., 2012). This could explain the high nitrogen removal efficiency of the CW-MFC.

5 Conclusion

Compared with the CW system, the CW-MFC system improved the removal efficiency of pollutants in Cr(VI) wastewater while generating electricity. Most of the Cr in the substrate and *L. hexandra* was reduced to the less toxic Cr(III), and the CW-MFC system could better promote the migration and transformation of Cr compared to the CW system. The abundance of electrogenic bacteria Geobacter and metal dissimilatory reducing bacteria *Acinetobacter* in CW-MFC is higher than that in CW. Thus, CW-MFC is an extremely cost effective and high-efficiency technology that can efficiently remove and detoxify Cr(VI). To summarize, these research results are expected to provide a scientific basis for improving the treatment performance of Cr(VI) wastewater using CW-MFC systems.

Data availability statement

The raw data supporting the conclusion of this article will be made available by the authors, without undue reservation.

Author contributions

Funding acquisition: SY; Investigation: PJ; Resources: ZD; Data curation: GT; Writing and Editing: YS. All authors have read and agreed to the published version of the manuscript

Funding

This work was funded by the Natural Science Foundation of China (51868010 and 52170154), Guangxi Natural Science Foundation Program (2019GXNSFBA245083 and 2021GXNSFBA196023), and the Innovation Project of Guangxi Graduate Education (YCBZ2021066). This work was supported by the Collaborative Innovation Center for Exploration of Hidden Nonferrous Metal Deposits and Development of New Materials in Guangxi.

Conflict of interest

The authors declare that the research was conducted in the absence of any commercial or financial relationships that could be construed as a potential conflict of interest.

Publisher's note

All claims expressed in this article are solely those of the authors and do not necessarily represent those of their affiliated organizations, or those of the publisher, the editors and the reviewers. Any product that may be evaluated in this article, or claim that may be made by its manufacturer, is not guaranteed or endorsed by the publisher.

RETRACTED

References

Adam, M. R., Salleh, N. M., Othman, M. H. D., Matsuura, T., Ali, M. H., Puteh, M. H., et al. (2018). The adsorptive removal of chromium (VI) in aqueous solution by novel natural zeolite based hollow fibre ceramic membrane. *J. Environ. Manag.* 224, 252–262. doi:10.1016/j.jenvman.2018.07.043

Augustynowicz, J., Kołton, A. M., Baran, A. M., Kostecka-Gugała, A. M., and Lasek, W. W. (2013). Strategy of Cr detoxification by Callitriche cophocarpa. *Open Chem.* 11 (2), 295–303. doi:10.2478/s11532-012-0161-8

Augustynowicz, J., Lekka, M. B., and Wróbel, P. M. (2014). Mechanical properties of Callitriche cophocarpa leaves under Cr(VI)/Cr(III) influence. *Acta Physiol. Plant.* 36 (8), 2025–2032. doi:10.1007/s11738-014-1580-2

Barrera-Díaz, C. E., Lugo-Lugo, V., and Bilyeu, B. (2012). A review of chemical, electrochemical and biological methods for aqueous Cr(VI) reduction. *J. Hazard. Mater.* 223 (2), 1–12. doi:10.1016/j.jhazmat.2012.04.054

Blowes, D. (2002). Tracking hexavalent Cr in groundwater. *Sci. (New York, N.Y.)* 295, 2024–2025. doi:10.1126/science.1070031

Broadway, A., Cave, M. R., Wragg, J., Fordyce, F. M., Bewley, R. J. F., Graham, M. C., et al. (2010). Determination of the bioaccessibility of chromium in Glasgow soil and the implications for human health risk assessment. *Sci. Total Environ.* 409 (2), 267–277. doi:10.1016/j.scitotenv.2010.09.007

Chaudhry, S. A., Khan, T. A., and Ali, I. (2017). Equilibrium, kinetic and thermodynamic studies of Cr(VI) adsorption from aqueous solution onto manganese oxide coated sand grain (MOCSG). *J. Mol. Liq.* 236, 320–330. doi:10.1016/j.molliq.2017.04.029

Chen, Y., Shi, J., Rong, H., Zhou, X., Chen, F., Li, X., et al. (2020). Adsorption mechanism of lead ions on porous ceramsite prepared by co-combustion ash of sewage sludge and biomass. *Sci. Total Environ.* 702, 135017. doi:10.1016/j.scitotenv.2019.135017

Cheng, D., Ngo, H. H., Guo, W., Chang, S. W., Nguyen, D. D., Liu, Y., et al. (2021). Evaluation of a continuous flow microbial fuel cell for treating synthetic swine wastewater containing antibiotics. *Sci. Total Environ.* 756, 144133. doi:10.1016/j.scitotenv.2020.144133

Choi, C., and Cui, Y. (2012). Recovery of silver from wastewater coupled with power generation using a microbial fuel cell. *Bioresour. Technol.* 107, 522–525. doi:10.1016/j.biortech.2011.12.058

Dermou, E., Velissariou, A., Xenos, D., and Vayenas, D. V. (2005). Biological chromium(VI) reduction using a trickling filter. *J. Hazard. Mater.* 126 (1), 78–85. doi:10.1016/j.jhazmat.2005.06.008

Dharnaik, A. S., and Ghosh, P. K. (2014). Hexavalent chromium [Cr(VI)] removal by the electrochemical ion-exchange process. *Environ. Technol.* 35 (18), 2272–2279. doi:10.1080/09593330.2014.902108

Di, L., Li, Y., Nie, L., Wang, S., and Kong, F. (2020). Influence of plant radial oxygen loss in constructed wetland combined with microbial fuel cell on nitrobenzene removal from aqueous solution. *J. Hazard. Mater.* 394, 122542. doi:10.1016/j.jhazmat.2020.122542

Dotro, G., Castro, S., Tujchneider, O., Piovano, N., Paris, M., Faggi, A., et al. (2012). Performance of pilot-scale constructed wetlands for secondary treatment of chromium-bearing tannery wastewaters. *J. Hazard. Mater.* 239-240, 142–151. doi:10.1016/j.jhazmat.2012.08.050

Dubey, S., Misra, P., Dwivedi, S., Chatterjee, S., Bag, S. K., Mantri, S., et al. (2010). Transcriptomic and metabolomic shifts in rice roots in response to Cr (VI) stress. *BMC Genomics* 11 (1), 648. doi:10.1186/1471-2164-11-648

Espinoza-Quiñones, F., Martin, N., Stutz, G., Tirao, G., Módenes, A., Palácio, S., et al. (2008). *Hexavalent chromium detoxification by three species of aquatic macrophytes*.

Gil-Cardeza, M. L., Ferri, A., Cornejo, P., and Gomez, E. (2014). Distribution of chromium species in a Cr-polluted soil: Presence of Cr(III) in glomalin related protein fraction. *Sci. Total Environ.* 493, 828–833. doi:10.1016/j.scitotenv.2014.06.080

Gomes, A. C., Silva, L., Albuquerque, A., Simões, R., and Stefanakis, A. I. (2018). Investigation of lab-scale horizontal subsurface flow constructed wetlands treating industrial cork boiling wastewater. *Chemosphere* 207, 430–439. doi:10.1016/j.chemosphere.2018.05.123

Gorby, Y., Yanina, S., McLean, J., Rosso, K., Moyles, D., Dohnalkova, A., et al. (2006). Electrically conductive bacterial nanowires produced by shewanella oneidensis strain MR-1 and other microorganisms. *Proc. Natl. Acad. Sci. U. S. A.* 103, 11358–11363. doi:10.1073/pnas.0604517103

Gul, H., Raza, W., Lee, J., Azam, M., Ashraf, M., and Kim, K.-H. (2021a). Progress in microbial fuel cell technology for wastewater treatment and energy harvesting. *Chemosphere* 281, 130828. doi:10.1016/j.chemosphere.2021.130828

Gul, P., Ahmad, K. S., and Ali, D. (2021b). Activated carbon processed from Citrus sinensis: Synthesis, characterization and application for adsorption-based separation of toxic pesticides from soils. *Sep. Sci. Technol.* 56 (12), 2026–2035. doi:10.1080/01496395.2020.1810071

Gupta, S., Srivastava, P., Patil, S. A., and Yadav, A. K. (2021). A comprehensive review on emerging constructed wetland coupled microbial fuel cell technology: Potential applications and challenges. *Bioresour. Technol.* 320, 124376. doi:10.1016/j.biortech.2020.124376

Gupta, S., Yadav, A., and Verma, N. (2017). Simultaneous Cr(VI) reduction and bioelectricity generation using microbial fuel cell based on alumina-nickel nanoparticles-dispersed carbon nanofiber electrode. *Chem. Eng. J.* 307, 729–738. doi:10.1016/j.cej.2016.08.130

Habibul, N., Hu, Y., Wang, Y.-K., Chen, W., Yu, H.-Q., and Sheng, G.-P. (2016). Bioelectrochemical chromium(VI) removal in plant-microbial fuel cells. *Environ. Sci. Technol.* 50 (7), 3882–3889. doi:10.1021/acs.est.5b06376

Han, Y.-L., Huang, S.-Z., Gu, J.-G., Qiu, S., and Chen, J.-M. (2008). Tolerance and accumulation of lead by species of Iris L. *Ecotoxicology* 17 (8), 853–859. doi:10.1007/s10646-008-0248-3

Hanumantu, J. R. (2021). Characterization studies on adsorption of lead and cadmium using activated carbon prepared from waste tyres. *Nat. Environ. Pollut. Technol.* 20. doi:10.46488/NEPT.2021.v20i02.012

Hartl, M., Bedoya-Ríos, D. F., Fernández-Gatell, M., Rousseau, D. P. L., Du Laing, G., Garfí, M., et al. (2019). Contaminants removal and bacterial activity enhancement along the flow path of constructed wetland microbial fuel cells. *Sci. Total Environ.* 652, 1195–1208. doi:10.1016/j.scitotenv.2018.10.234

Howe, J. A., Loeppert, R. H., DeRose, V. J., Hunter, D. B., and Bertsch, P. M. (2003). Localization and speciation of chromium in subterranean clover using XRF, XANES, and EPR spectroscopy. *Environ. Sci. Technol.* 37 (18), 4091–4097. doi:10.1021/es034156l

Jain, M., Garg, V. K., and Kadirvelu, K. (2010). Adsorption of hexavalent chromium from aqueous medium onto carbonaceous adsorbents prepared from waste biomass. *J. Environ. Manag.* 91 (4), 949–957. doi:10.1016/j.jenvman.2009.12.002

Jiang, D., Li, B., Jia, W., and Lei, Y. (2009). Effect of inoculum types on bacterial adhesion and power production in microbial fuel cells. *Appl. Biochem. Biotechnol.* 160 (1), 182–196. doi:10.1007/s12010-009-8541-z

Kazemi, M., Jahanshahi, M., and Peyravi, M. (2018). Hexavalent chromium removal by multilayer membrane assisted by photocatalytic couple nanoparticle from both permeate and retentate. *J. Hazard. Mater.* 344, 12–22. doi:10.1016/j.jhazmat.2017.09.059

Kotaś, J., and Stasicka, Z. (2000). Chromium occurrence in the environment and methods of its speciation. *Environ. Pollut.* 107 (3), 263–283. doi:10.1016/S0269-7491(99)00168-2

Li, H., Wang, B., Deng, S., Dai, J., and Shao, S. (2019). Oxygen-containing functional groups on bioelectrode surface enhance expression of c-type cytochromes in biofilm and boost extracellular electron transfer. *Bioresour. Technol.* 292, 121995. doi:10.1016/j.biortech.2019.121995

Li, M., and Zhou, S. (2018). α-Fe2O3/polyaniline nanocomposites as an effective catalyst for improving the electrochemical performance of microbial fuel cell. *Chem. Eng. J.* 339, 539–546. doi:10.1016/j.cej.2018.02.002

Li, M., Zhou, S., Xu, Y., Liu, Z., Ma, F., Zhi, L., et al. (2018). Simultaneous Cr(VI) reduction and bioelectricity generation in a dual chamber microbial fuel cell. *Chem. Eng. J.* 334, 1621–1629. doi:10.1016/j.cej.2017.11.144

Li, Y., Jin, Z., Li, T., and Xiu, Z. (2012). One-step synthesis and characterization of core-shell Fe@SiO2 nanocomposite for Cr (VI) reduction. *Sci. Total Environ.* 421-422, 260–266. doi:10.1016/j.scitotenv.2012.01.010

Lim, S.-F., Zheng, Y.-M., Zou, S.-W., and Chen, J. P. (2008). Characterization of copper adsorption onto an alginate encapsulated magnetic sorbent by a combined FT-IR, XPS, and mathematical modeling study. *Environ. Sci. Technol.* 42 (7), 2551–2556. doi:10.1021/es7021889

Liu, J., Zhang, X.-h., You, S.-h., Wu, Q.-x., Chen, S.-m., and Zhou, K.-n. (2014). Cr(VI) removal and detoxification in constructed wetlands planted with Leersia hexandra Swartz. *Ecol. Eng.* 71, 36–40. doi:10.1016/j.ecoleng.2014.07.047

Liu, S., Qiu, D., Lu, F., Wang, Y., Wang, Z., Feng, X., et al. (2022). Acorus calamus L. constructed wetland-microbial fuel cell for Cr(VI)-containing wastewater treatment and bioelectricity production. *J. Environ. Chem. Eng.* 10 (3), 107801. doi:10.1016/j.jece.2022.107801

Logan, B. E., and Regan, J. M. (2006). Electricity-producing bacterial communities in microbial fuel cells. *Trends Microbiol.* 14 (12), 512–518. doi:10.1016/j.tim.2006.10.003

RETRACTED

Moreau, J., Fournelle, J., and Banfield, J. (2013). Quantifying heavy metals sequestration by sulfate-reducing bacteria in an acid mine drainage-contaminated natural wetland. *Front. Microbiol.* 4, 43. doi:10.3389/fmicb.2013.00043

Mousavi, S., Ibrahim, S., Aroua, M. K., and Ghafari, S. (2012). Development of nitrate elimination by autohydrogenotrophic bacteria in bio-electrochemical reactors – a review. *Biochem. Eng. J.* 67, 251–264. doi:10.1016/j.bej.2012.04.016

Mu, C., Wang, L., and Wang, L. (2020). Performance of lab-scale microbial fuel cell coupled with unplanted constructed wetland for hexavalent chromium removal and electricity production. *Environ. Sci. Pollut. Res.* 27 (20), 25140–25148. doi:10.1007/s11356-020-08982-z

Obata, O., Greenman, J., Kurt, H., Chandran, K., and Ieropoulos, I. (2020). Resilience and limitations of MFC anodic community when exposed to antibacterial agents. *Bioelectrochemistry* 134, 107500. doi:10.1016/j.bioelechem.2020.107500

Padmavathiamma, P., and Li, L. (2007). Phytoremediation technology: Hyper-accumulation metals in plants. *Water Air Soil Pollut.* 184, 105–126. doi:10.1007/s11270-007-9401-5

Pradhan, D., Sukla, L. B., Sawyer, M., and Rahman, P. K. S. M. (2017). Recent bioreduction of hexavalent chromium in wastewater treatment: A review. *J. Industrial Eng. Chem.* 55, 1–20. doi:10.1016/j.jiec.2017.06.040

Qin, N., Zhang, Y., Zhou, H., Geng, Z., Liu, G., Zhang, Y., et al. (2016). Enhanced removal of trace Cr(VI) from neutral and alkaline aqueous solution by FeCo bimetallic nanoparticles. *J. Colloid Interface Sci.* 472, 8–15. doi:10.1016/j.jcis.2016.03.025

Reguera, G., McCarthy, K. D., Mehta, T., Nicoll, J. S., Tuominen, M. T., and Lovley, D. R. (2005). Extracellular electron transfer via microbial nanowires. *Nature* 435 (7045), 1098–1101. doi:10.1038/nature03661

Ren, G., Sun, Y., Lu, A., Li, Y., and Ding, H. (2018). Boosting electricity generation and Cr(VI) reduction based on a novel silicon solar cell coupled double-anode (photoanode/bioanode) microbial fuel cell. *J. Power Sources* 408, 46–50. doi:10.1016/j.jpowsour.2018.10.081

Ren, Z., Xu, X., Wang, X., Gao, B., Yue, Q., Song, W., et al. (2016). FTIR, Raman, and XPS analysis during phosphate, nitrate and Cr(VI) removal by amine cross-linking biosorbent. *J. Colloid Interface Sci.* 468, 313–323. doi:10.1016/j.jcis.2016.01.079

Römheld, V. (1991). The role of phytosiderophores in acquisition of iron and other micronutrients in graminaceous species: An ecological approach. *Plant Soil* 130 (1), 127–134. doi:10.1007/BF00011867

Sinha, V., Manikandan, N. A., Pakshirajan, K., and Chaturvedi, R. (2017). Continuous removal of Cr(VI) from wastewater by phytoextraction using Tradescantia pallida plant based vertical subsurface flow constructed wetland system. *Int. Biodeterior. Biodegrad.* 119, 96–103. doi:10.1016/j.ibiod.2016.10.003

Srivastava, P., Abbassi, R., Garaniya, V., Lewis, T., and Yadav, A. K. (2020a). Performance of pilot-scale horizontal subsurface flow constructed wetland coupled with a microbial fuel cell for treating wastewater. *J. Water Process Eng.* 33, 100994. doi:10.1016/j.jwpe.2019.100994

Srivastava, P., Abbassi, R., Kumar Yadav, A., Garaniya, V., Kumar, N., Khan, S. J., et al. (2020b). Enhanced chromium(VI) treatment in electroactive constructed wetlands: Influence of conductive material. *J. Hazard. Mater.* 387, 121722. doi:10.1016/j.jhazmat.2019.121722

Sun, Y., Yue, Q., Mao, Y., Gao, B., Gao, Y., and Huang, L. (2014). Enhanced adsorption of chromium onto activated carbon by microwave-assisted H3PO4 mixed with Fe/Al/Mn activation. *J. Hazard. Mater.* 265, 191–200. doi:10.1016/j.jhazmat.2013.11.057

Tao, H.-C., Liang, M., Li, W., Zhang, L.-J., Ni, J.-R., and Wu, W.-M. (2011). Removal of copper from aqueous solution by electrodeposition in cathode chamber of microbial fuel cell. *J. Hazard. Mater.* 189 (1), 186–192. doi:10.1016/j.jhazmat.2011.02.018

Tao, M., Guan, L., Jing, Z., Tao, Z., Wang, Y., Luo, H., et al. (2020). Enhanced denitrification and power generation of municipal wastewater treatment plants (WWTPs) effluents with biomass in microbial fuel cell coupled with constructed wetland. *Sci. Total Environ.* 709, 136159. doi:10.1016/j.scitotenv.2019.136159

Torresi, E., Escolà Casas, M., Polesel, F., Plósz, B. G., Christensson, M., and Bester, K. (2017). Impact of external carbon dose on the removal of micropollutants using methanol and ethanol in post-denitrifying Moving Bed Biofilm Reactors. *Water Res.* 108, 95–105. doi:10.1016/j.watres.2016.10.068

Uddin, M. J., Jeong, Y.-K., and Lee, W. (2021). Microbial fuel cells for bioelectricity generation through reduction of hexavalent chromium in wastewater: A review. *Int. J. Hydrogen Energy* 46 (20), 11458–11481. doi:10.1016/j.ijhydene.2020.06.134

Vendruscolo, F., da Rocha Ferreira, G. L., and Antoniosi Filho, N. R. (2017). Biosorption of hexavalent chromium by microorganisms. *Int. Biodeterior. Biodegrad.* 119, 87–95. doi:10.1016/j.ibiod.2016.10.008

Wang, J., Deng, H., Wu, S.-S., Deng, Y.-C., Liu, L., Han, C., et al. (2019). Assessment of abundance and diversity of exoelectrogenic bacteria in soil under different land use types. *CATENA* 172, 572–580. doi:10.1016/j.catena.2018.09.028

Wang, L., Xu, D., Zhang, Q., Liu, T., and Tao, Z. (2022). Simultaneous removal of heavy metals and bioelectricity generation in microbial fuel cell coupled with constructed wetland: An optimization study on substrate and plant types. *Environ. Sci. Pollut. Res.* 29 (1), 768–778. doi:10.1007/s11356-021-15688-3

Wang, Z., Lim, B., and Choi, C. (2011). Removal of Hg2+ as an electron acceptor coupled with power generation using a microbial fuel cell. *Bioresour. Technol.* 102 (10), 6304–6307. doi:10.1016/j.biortech.2011.02.027

Xie, B., Gong, W., Ding, A., Yu, H., Qu, F., Tang, X., et al. (2017). Microbial community composition and electricity generation in cattle manure slurry treatment using microbial fuel cells: Effects of inoculum addition. *Environ. Sci. Pollut. Res.* 24 (29), 23226–23235. doi:10.1007/s11356-017-9959-4

Yadav, A. K., Dash, P., Mohanty, A., Abbassi, R., and Mishra, B. K. (2012). Performance assessment of innovative constructed wetland-microbial fuel cell for electricity production and dye removal. *Ecol. Eng.* 47, 126–131. doi:10.1016/j.ecoleng.2012.06.029

Yangdong, O., Liwen, G., and hongcui, M. (2012). Research on the influence of oxygen-containing functional group and gas emission by coal seams. *Energy Procedia* 17, 1901–1906. doi:10.1016/j.egypro.2012.02.330

Zhao, C., Shang, D., Zou, Y., Du, Y., Wang, Q., Xu, F., et al. (2020). Changes in electricity production and microbial community evolution in constructed wetland-microbial fuel cell exposed to wastewater containing Pb(II). *Sci. Total Environ.* 732, 139127. doi:10.1016/j.scitotenv.2020.139127

Zheng, Q., Na, S., Li, X., Li, N., Hai, R., and Wang, X. (2019). Acute effects of hexavalent chromium on the performance and microbial community of activated sludge in aerobiotic reactors. *Environ. Technol.* 40 (14), 1871–1880. doi:10.1080/09593330.2018.1432695

Zhou, Y., Xu, D., Xiao, E., Xu, D., Xu, P., Zhang, X., et al. (2017). Relationship between electrogenic performance and physiological change of four wetland plants in constructed wetland-microbial fuel cells during non-growing seasons. *J. Environ. Sci.* 70, 54–62. doi:10.1016/j.jes.2017.11.008

Zongo, I., Leclerc, J.-P., Maïga, H. A., Wéthé, J., and Lapicque, F. (2009). Removal of hexavalent chromium from industrial wastewater by electrocoagulation: A comprehensive comparison of aluminium and iron electrodes. *Sep. Purif. Technol.* 66 (1), 159–166. doi:10.1016/j.seppur.2008.11.012

RETRACTED